Article

Cite This: Biomacromolecules 2018, 19, 3766−3775

pubs.acs.org/Biomac

Native Chemical Ligation for Cross-Linking of Flower-Like Micelles

Marzieh Najafi,[†] Neda Kordalivand,[†] Mohammad-Amin Moradi,[‡,§] Joep van den Dikkenberg,[†] Remco Fokkink,[∥] Heiner Friedrich,[‡,§] Nico A. J. M. Sommerdijk,[‡,§] Mathew Hembury,[†] and Tina Vermonden*[,†]

[†]Department of Pharmaceutics, Utrecht Institute for Pharmaceutical Sciences (UIPS), Science for Life, Faculty of Science, Utrecht University, P.O. Box 80082, 3508 TB Utrecht, The Netherlands

[‡]Laboratory of Materials and Interface Chemistry and Centre for Multiscale Electron Microscopy Department of Chemical Engineering and Chemistry, Eindhoven University of Technology, Eindhoven, 5600 MB, The Netherlands

[§]Institute for Complex Molecular Systems, Eindhoven University of Technology, Eindhoven, 5600 MB, The Netherlands

[∥]Physical Chemistry and Soft Matter, Wageningen University and Research, Stippeneng 4, 6708 WE Wageningen, The Netherlands

Supporting Information

ABSTRACT: In this study, native chemical ligation (NCL) was used as a selective cross-linking method to form core-cross-linked thermosensitive polymeric micelles for drug delivery applications. To this end, two complementary ABA triblock copolymers having polyethylene glycol (PEG) as midblock were synthesized by atom transfer radical polymerization (ATRP). The thermosensitive poly isopropylacrylamide (PNIPAM) outer blocks of the polymers were copolymerized with either *N*-(2-hydroxypropyl)-methacrylamide-cysteine (HPMA-Cys), P(NIPAM-*co*-HPMA-Cys)-PEG-P(NIPAM-*co*-HPMA-Cys) (PNC) or *N*-(2-hydroxypropyl)methacrylamide-ethylthioglycolate succinic acid (HPMA-ETSA), P(NIPAM-*co*-HPMA-ETSA)-PEG-P-(NIPAM-*co*-HPMA-ETSA) (PNE). Mixing of these polymers in aqueous solution followed by heating to 50 °C resulted in the formation of thermosensitive flower-like micelles. Subsequently, native chemical ligation in the core of micelles resulted in stabilization of the micelles with a *Z*-average of 65 nm at body temperature. Decreasing the temperature to 10 °C only affected the size of the micelles (increased to 90 nm) but hardly affected the polydispersity index (PDI) and aggregation number (N_{agg}) confirming covalent stabilization of the micelles by NCL. CryoTEM images showed micelles with an uniform spherical shape and dark patches close to the corona of micelles were observed in the tomographic view. The dark patches represent more dense areas in the micelles which coincide with the higher content of HPMA-Cys/ETSA close to the PEG chain revealed by the polymerization kinetics study. Notably, this cross-linking method provides the possibility for conjugation of functional molecules either by using the thiol moieties still present after NCL or by simply adjusting the molar ratio between the polymers (resulting in excess cysteine or thioester moieties) during micelle formation. Furthermore, in vitro cell experiments demonstrated that fluorescently labeled micelles were successfully taken up by HeLa cells while cell viability remained high even at high micelle concentrations. These results demonstrate the potential of these micelles for drug delivery applications.

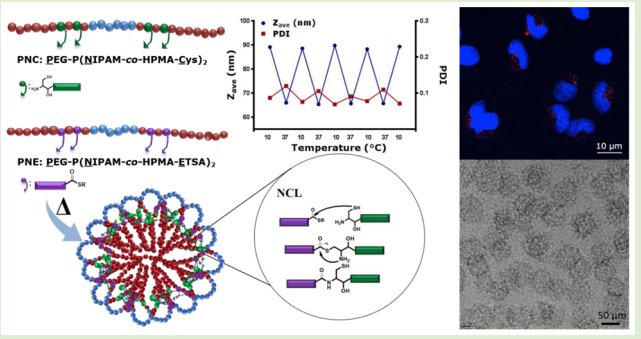

INTRODUCTION

Polymeric micelles (PM) can be formed by amphiphilic block copolymers and have been studied extensively to improve delivery of mainly hydrophobic drugs.[1,2] In aqueous media, at concentrations above the critical micelle concentration (CMC), amphiphilic block copolymers (AB or ABA) self-assemble into nanosized particles. While AB polymers self-assemble into star-like micelles, ABA triblock copolymers with a hydrophilic midblock (B) are capable of self-assembling into so-called flower-like micelles.[3−5] Although flower-like micelles share many characteristics with star-like micelles, they have been reported to have some advantageous properties regarding lower CMC and higher stability.[6−8]

The hydrophilic midblock (B block) in flower-like micelles is often composed of poly(ethylene glycol) (PEG).[6] Starting from this PEG midblock, there are several methods to synthesize ABA block copolymers among which atom transfer radical polymerization (ATRP) provides good control over the structure and sequence of monomers in a polymer.[9,10] ATRP conditions enable the growth of hydrophobic A-blocks with a desired length and tunable monomer composition.[11]

Received: June 11, 2018
Revised: August 9, 2018
Published: August 13, 2018

During micellization of ABA block polymers, in aqueous solution, the PEG block forms a looped structure of the hydrophilic corona surrounding the hydrophobic core composed of the self-assembled outer blocks.[3] The hydrophobic core has been used to solubilize hydrophobic drugs and the hydrophilic shell stabilizes micelles and enhances their circulation time in body fluids.[12,13] However, the equilibrium between micelles and unimers is highly affected by dilution and at concentrations below the CMC, micelles start to dissociate. This dissociation can lead to premature release of a loaded drug from the micelles upon administration in, for example, the circulation.[14] Moreover, proteins present in the body can extract drugs from micellar formulations. To enhance the in vivo stability of micelles, several methods have been developed, including the frequently applied method of core cross-linking and covalent linking of drugs to the polymers present in the micelles.[15]

For covalent cross-linking of the micellar core, the reactive groups should be located in the hydrophobic block of the polymers. Of course, it is important that the chemical properties of these functional groups do not hamper micelle formation. A commonly applied method for core cross-linking of micelles makes use of radical polymerization. In this method, polymerizable groups such as methacrylates or acrylates are introduced in the hydrophobic block of amphiphilic polymers, which are located in the core of the micelles after micellization. Subsequently, by UV illumination in the presence of a photoinitiator or by thermal radical polymerization, these functional groups can be cross-linked in the core of these types of micelles.[16,8] Another common method for covalent cross-linking of micelles is introducing reactive groups, such as epoxy or acidic moieties in the side chain of amphiphilic polymers that are subsequently cross-linked by a bifunctional molecule, such as a diamine.[17,18] Also, disulfide bridges as cross-links can be introduced by using cystamine in the micellar core, which gives the micelles triggered release properties interesting for compounds that need to be delivered intracellularly. These disulfide bridges will be broken in the intracellular reducing environment.[19,20] Also, free thiols in the hydrophobic block of the amphiphilic polymer can be used for disulfide core cross-linking; however, oxidative conditions should be provided.[21,22] Recently, "click" reactions received attention for cross-linking of polymeric micelles.[23,24] Several studies reported the formation of cross-linked micelles and nanoparticles using copper-catalyzed alkyne−azide cycloaddition reaction (CuAAC).[25,26] For example, redox-responsive core cross-linked micelles were synthesized using bis(azidoethyl) disulfide as a redox-responsive cross-linker.[27] Other studies used Diels−Alder reactions for cross-linking, for example, formation of star-like micelles by cross-linking block copolymers having furan functionalities using bismaleimide cross-linkers in tetrahydrofuran (THF).[28] Furthermore, PEG-polyester type polymers with pending mercapto groups were cross-linked via a thiol−ene "click" chemistry approach using a diacrylate cross-linker.[29]

Besides all the developments in this field, many of the applied cross-linking methods suffer from some limitations (e.g., exposure to radicals, oxidative conditions, use of (toxic) catalysts which mostly require an inert environment, or use of organic solvents), that can potentially damage the cargo of the micelles. Furthermore, the functional groups used in these methods will be consumed during cross-linking and cannot be used for further modification steps. Therefore, introducing a cross-linking method that is not only applicable in aqueous solutions but also retains its reactive groups in the micellar core after cross-linking is of high interest. Among chemical conjugation methods performed in aqueous solution, native chemical ligation,[30] a chemoselective method, has been studied for cross-linking of hydrogels.[31−33] However, this cross-linking method has not been applied yet for core-cross-linking of micelles. Native chemical ligation involves nucleophilic attack of the thiol group of an *N*-terminal cysteine to a thioester moiety. The obtained thioester intermediate rearranges by an intramolecular *S*,*N*-acyl shift that results in the formation of an amide. Notably, after the *S*,*N*-acyl shift a free thiol moiety remains available, which offers the possibility to further conjugate desirable molecules via, for example, a disulfide bond.

The goal of this study was to investigate native chemical ligation as a selective reaction that occurs in water for core cross-linking of flower-like micelles.[34] For this purpose, an ABA triblock copolymer consisting of polyethylene glycol (PEG) as midblock and thermosensitive poly *N*-isopropylacrylamide (NIPAM)-*co*-*N*-(2-hydroxypropyl)methacrylamide-cysteine (HPMA-Cys) as outer blocks P(NIPAM-*co*-HPMA-Cys)-PEG-P(NIPAM-*co*-HPMA-Cys) (PNC)) was synthesized by ATRP. A complementary polymer, P(NIPAM-*co*-HPMA-ETSA)-PEG-P(NIPAM-*co*-HPMA-ETSA) (PNE), containing a novel monomer of *N*-(2-hydroxypropyl)-methacrylamide-ethylthioglycolate succinic acid (HPMA-ETSA) carrying a thioester moiety, was developed. In these amphiphilic polymers designed to self-assemble into micelles, the PEG block represents the hydrophilic part, PNIPAM blocks initiate micellization in aqueous solution by increasing temperature and HPMA-Cys/ETSA monomers provide *N*-terminal cysteine and thioester functionalities for NCL cross-linking to stabilize the micellar structure. Upon mixing of the polymers in aqueous solution, the presence of PNIPAM thermosensitive blocks allows micelle formation by increasing the temperature above the lower critical solution temperature (LCST) of these polymers.[35] The stability of the micelles after covalent cross-linking by NCL was investigated by lowering the temperature of the micellar solution below the LCST of the polymers. In addition, the shape and conformation of micelles were studied by static light scattering and CryoTEM. To investigate cytocompatibility for potential biomedical applications of the obtained micelles, a cytotoxicity assay was performed. Moreover, cellular uptake of labeled micelles was studied using A549 (human lung carcinoma cell line) and HeLa (human epithelial cervix carcinoma cell line) cells.

MATERIALS AND METHODS

All commercial chemicals were obtained from Sigma-Aldrich (Zwijndrecht, The Netherlands) and used as received unless indicated otherwise. *N*-(2-Hydroxypropyl)methacrylamide (HPMA) was synthesized by a reaction of methacryloyl chloride with 1-aminopropan-2-ol in dichloromethane according to a literature procedure.[36] Peptide grade dichloromethane (CH_2Cl_2) was obtained from Biosolve (Valkenswaard, The Netherlands). *N*,*N*′-Dimethylaminopyridine (DMAP) was purchased from Fluka (Zwijndrecht, The Netherlands). Boc-*S*-acetamidomethyl-L-cysteine (Boc-Cys(Acm)-OH was purchased from Bachem (Bubendorf, Switzerland). *N*-(2-Hydroxypropyl)methacrylamide-Boc-*S*-acetamidomethyl-L-cysteine (HPMA-Boc-Cys(Acm)) was synthesized as described by Boere et al.[33] Ethylthioglycolate succinic acid (ETSA) was prepared according to a literature procedure.[31] Phosphate buffered saline (PBS) pH 7.4 (8.2 g/L NaCl, 3.1 g/L $Na_2HPO_4{\cdot}12H_2O$, 0.3 g/L $NaH_2PO_4{\cdot}2H_2O$)

DOI: 10.1021/acs.biomac.8b00908
Biomacromolecules 2018, 19, 3766−3775

was purchased from B. Braun (Melsungen, Germany). Celltiter AQ-MTS (3-(4,5-dimethylthiazol-2-yl)-5-(3-carboxymethoxyphenyl)-2-(4-sulfophenyl)-2H-tetrazolium) #3580 and Lysis Solution #G182A were purchased from Promega (U.S.A.). NHS-Alexa Fluor 647 and maleimide-Alexa flour C5 568 fluorescent dyes were obtained from Invitrogen (Eugene, OR, U.S.A.).

Synthesis of Poly(ethylene glycol) Bis(2-bromoisobutyrate). The synthesis of a PEG macroinitiator was achieved according to a method previously reported[3] with slight modifications. Briefly, dried PEG 6 kDa (5 gr) was dissolved in 70 mL of dry THF and purged with nitrogen. To this solution, triethylamine (0.7 mL) and α-bromoisobutyryl bromide (0.6 mL) were added, and the reaction mixture was stirred overnight at room temperature. Next, the formed bromide salt was filtered off and subsequently, THF was evaporated under reduced pressure. The crude product was dialyzed against water for 2 days and afterward lyophilized. The degree of functionalization was determined by addition of trichloroacetyl isocyanate (TAIC) reacting with unmodified OH groups.[37] ^{1}H NMR analysis confirmed the formation of a fully functionalized PEG ATRP macroinitiator. ^{1}H NMR ($CDCl_3$): δ 4.3 (t, 4H, OCH_2), 3.85 (t, 4H, OCH_2), 3.65 (t, 531H, OCH_2), 3.35 (t, 4H, OCH_2), 1.85 ppm (s, 12H, CCH_3).

Synthesis of *N*-(2-Hydroxypropyl) Methacrylamide-Ethylthioglycolate Succinic Acid (HPMA-ETSA). In a typical procedure, ethylthioglycolate succinic acid (ETSA; 1.54 g, 7 mmol), HPMA (1.00 g, 7 mmol), and DMAP (85 mg, 7 μmol) were dissolved in dry CH_2Cl_2 (7 mL). To this solution, *N*,*N*′-dicyclohexylcarbodiimide (DCC; 1.44 g, 7 mmol) was added, and the reaction mixture was stirred for 16 h under a nitrogen atmosphere at room temperature. Subsequently, the suspension was cooled to 0 °C and filtered, after which the filtrate was concentrated. The crude product was purified by silica gel chromatography, using CH_2Cl_2/CH_3OH (9:1 v/v) as eluent. The monomer HPMA-ETSA was obtained as milky oil with a yield of 57%. ^{1}H NMR ($CDCl_3$): δ 6.28 (s, 1H, N*H*), 5.68 (s, 1H, H_2C═CH), 5.31 (s, 1H, H_2C═CH), 5.05 (m, 1H, $CH_2CH(CH_3)$-O), 4.16 (q, 2H, CH_3CH_2O), 3.67 (d, 2H, $C(O)SCH_2C(O)$), 3.56 (dd, 1H, $NHCH_2CH(CH_3)O$), 3.32 (dd, 1H, $NHCH_2CH(CH_3)O$), 2.95 (t, 2H, $SC(O)CH_2CH_2$), 2.63 (t, 2H, $SC(O)CH_2CH_2$), 1.94 (s, 3H, $C═C(CH_3)$), 1.24 (m, 6H, CH_3CH_2O) and $NHCH_2CH(CH_3)$-O). ^{13}C NMR ($CDCl_3$): δ 196.5, 172.3, 171.3, 168.5, 139.8, 119.5, 70.7, 61.9, 44.0, 38.2, 31.2, 29.4, 18.9, 17.5, 14.0 (Supporting Information (SI), Figure 1)

Synthesis of P(NIPAM-*co*-HPMA-ETSA)-PEG-P(NIPAM-*co*-HPMA-ETSA), PNE. Poly(ethylene glycol) bis(2-bromoisobutyrate) (50 mg, 7.9 μmol), CuBr (4.5 mg, 0.031 mmol), $CuBr_2$ (4.7 mg, 0.021 mmol), NIPAM (268.9 mg; 2.3 mmol), and HPMA-ETSA (55 mg, 0.16 mmol) were dissolved in a mixture of 2.5 mL water and 2 mL ethanol. The mixture was stirred and deoxygenated by flushing with nitrogen for 15 min at room temperature, then placed in an ice bath for another 15 min. After addition of 16 μL (0.06 mmol) of tris[2-(dimethylamino)ethyl]amine (Me_6TREN) to the solution, the color of the mixture immediately changed to blue and the reaction was left for 5 h in an ice bath. The final product was dialyzed (cut off 10 kDa) against water at 4 °C for 1 day and lyophilized. The obtained polymer was characterized by GPC and ^{1}H NMR (SI, Figures 2 and 4A).

Synthesis of P(NIPAM-*co*-HPMA-Cys)-PEG-P(NIPAM-*co*-HPMA-Cys), PNC. Poly(ethylene glycol) bis(2-bromoisobutyrate) (50 mg, 7.9 μmol), CuBr (4.5 mg, 0.031 mmol), $CuBr_2$ (4.7 mg, 0.021 mmol), NIPAM (268.9 mg; 2.4 mmol), and HPMA-Boc-Cys(Acm) (67 mg, 0.16 mmol) were dissolved in a mixture of 3.5 mL of water and acetonitrile with a ratio of 3:1. The mixture was stirred and deoxygenated by flushing with nitrogen for 15 min at room temperature, then placed in an ice bath for another 15 min. After addition of 16 μL (0.06 mmol) of Me_6TREN to the solution, the color of the mixture immediately changed to blue and the reaction was left stirring for 2 h in an ice bath. The final product was dialyzed (cut off 10 kDa) against water at 4 °C for 1 day and subsequently lyophilized. The obtained polymer was characterized by GPC and ^{1}H NMR. To replace the bromide end groups, the obtained polymer was dissolved in 5 mL CH_2Cl_2 and treated with an excess (500 μL) of mercaptoethanol for 24 h. Next, the solvent was concentrated by evaporation and the pure polymer was obtained after precipitation in cold diethyl ether. Finally, the Acm and Boc protecting groups of cysteine were removed as explained previously.[32] The obtained polymer was characterized by GPC and ^{1}H NMR (SI, Figures 3 and 4B).

Kinetics of Polymerization. At several time points, 250 μL samples were taken from polymerization mixtures to monitor the conversion of polymerization by ^{1}H NMR and GPC. Samples of 50 μL were diluted with air-saturated $CDCl_3$ and analyzed by ^{1}H NMR. The integrals of signals at 5.5 and 5.30 ppm related to NIPAM and HPMA-Cys/ETSA, respectively, were compared to the PEG signal at 3.65 ppm as a reference. The remaining 200 μL was dialyzed against water for 1 day and then lyophilized. The dried product was dissolved in DMF/LiCl and the molecular weight was analyzed by GPC as described below.

NMR Spectroscopy. The obtained monomers, polymers, and micelles were studied by ^{1}H NMR (400 MHz) and ^{13}C NMR (100 MHz) measured on an Agilent 400-MR NMR spectrometer (Agilent Technologies, Santa Clara, U.S.A.). The chemical shifts were calibrated against residual solvent peaks of $CDCl_3$ (δ = 7.26 ppm), D_2O (δ = 4.79 ppm) for ^{1}H NMR, and δ = 77.16 ppm of $CDCl_3$ for ^{13}C NMR. Micelle solutions were analyzed on a Varian Inova 500 NMR instrument (Varian Inc., California, U.S.A.) in D_2O.

Gel Permeation Chromatography (GPC). To determine the molecular weight of polymers, GPC was performed on a Waters Alliance System (Waters Corporation, Milford, MA, U.S.A.) equipped with a refractive index detector using a Mixed-D column (Polymer Laboratories) at a temperature of 65 °C. The eluent consisting of 10 mM LiCl in DMF with a flow of 1 mL/min was used as mobile phase and samples were prepared in the same solvent at a concentration of 5 mg/mL. A series of linear PEGs with narrow and defined molecular weights were used as calibration standards.

Determination of Cloud Point. The cloud point (CP) of the obtained polymers was measured on a Jasco FP8300 spectrofluorometer (Tokyo, Japan) and excitation/emission wavelength was set at 650 nm. Polymers were dissolved at a concentration of 1 mg/mL in PBS and heated from 10 to 50 °C with a heating rate of 1 °C/min. The CP was defined as the onset of increasing scattering intensity.

Micelle Formation. Micelles were formed by a fast heating method as follows: PNC and PNE were dissolved separately in PBS at a concentration of 3 mg/mL at 4 °C. PNC and PNE polymers were mixed in a 1:1 mass ratio since they have equal molar ratios of HPMA-Cys and HPMA-ETSA and similar molecular weights. Subsequently, the mixed solution was quickly heated up to 50 °C using an oil bath and left at 50 °C for 3 h. Resulting micellar solutions were dialyzed against water for 2 days at room temperature and subsequently lyophilized. Micelles were characterized by DLS and NMR both before and after lyophilization.

CryoTEM. Transmission electron microscopy at cryogenic temperatures (CryoTEM) was done using the TU/e CryoTitan (FEI Company).[38] Graphene oxide grids, prepared by adding a single layer graphene sheet to a Quantifoil grid,[39] were used for sampling via an automated robot (Vitrobot Mark III, FEI Company), which was kept at room temperature. The excess of liquid sample on the grid was blotted away with filter paper to form a thin film of the dispersion. The thin layer of liquid on the grid was plunged rapidly into liquid ethane. The vitrification was done in 100% humidity atmosphere. A tilt series of 27 cryoTEM images from −65° to +65° with 5° steps were taken to reconstruct the 3D structure of the particles using IMOD via patch tracking alignment and AVIZO 9.0 software.[40]

Dynamic Light Scattering (DLS). The size of the micelles was measured by DLS on a Malvern CGS-3 goniometer (Malvern Ltd., Malvern, U.K.), ALV/LSE-5003 Correlator, and He−Ne 633 nm laser. All measurements were carried out at a 90° angle at temperatures of 10, 37, and 45 °C controlled by a thermostat water bath Julabo FS18. The solvent viscosity was corrected at each temperature by the software. The *Z*-average radius and polydispersity index was calculated by ALV and DTS software, respectively.

DOI: 10.1021/acs.biomac.8b00908
Biomacromolecules 2018, 19, 3766−3775

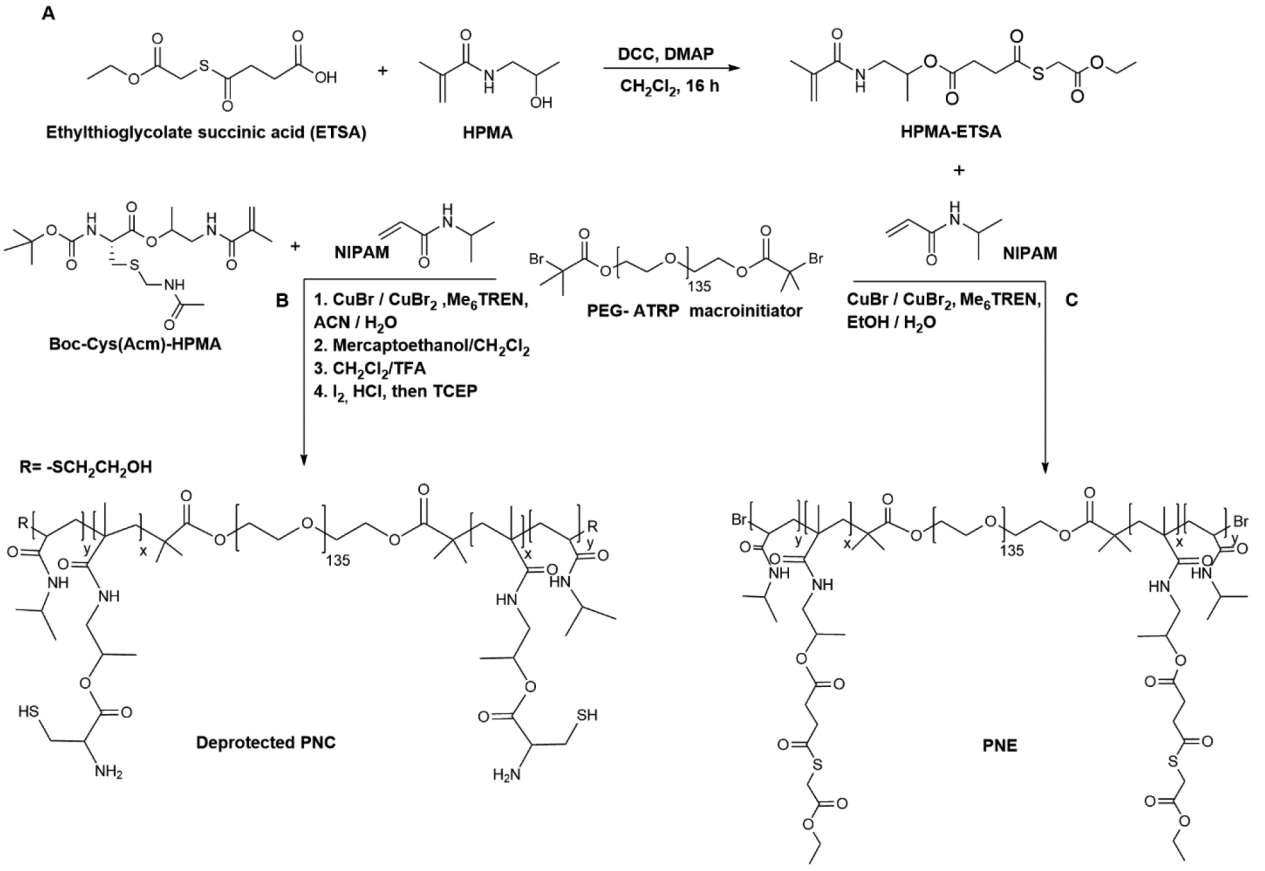

Figure 1. Synthesis route of (A) HPMA-ETSA and (B, C) ABA triblock copolymers containing PEG as midblocks and either copolymer of (B) NIPAM and HPMA-Boc-Cys(Acm) (PNC) or (C) NIPAM and HPMA-ETSA (PNE) as outer blocks.

Static Light Scattering (SLS). Weight-average molecular weight of the micelles and the radius of gyration were determined by SLS using an ALV7004 correlator, ALV/LSE-5004 Goniometer, ALV/Dual High QE APD detector unit with fiber splitting device with a setup of 2 off detection system and a Uniphase Model 1145P He−Ne Laser. The laser wavelength and power were set to 632.8 nm and 22 mW, respectively, and the temperature was controlled by a Julabo CF41 Thermostatic bath.

Ellman Assay. Ellman's reaction was performed on micelles to quantify the cross-link density in the micelles. Cysteine hydrochloride monohydrate standards were prepared at concentrations ranging from 0 to 1.5 mM in a 0.1 M sodium buffer/1 mM EDTA at pH 8.0. A HiTrap 1.5 mL, desalting column was equilibrated with the same buffer and was used for separation of micelles from ethyl thioglycolate. A stock solution of 4 mg/mL of Ellman's reagent was made and 50 μL was added to a mixture of 2.5 mL of buffer and 250 μL of each standard and ethyl thioglycolate sample. The thiol contents of samples were determined by measuring the absorbance at λ = 412 nm using a BMG spectrostar nano well plate reader.

Preparation of Fluorescently Labeled Micelles. To fluorescently label the micelles, micelles were formed following the same procedure as described above, then dialyzed and lyophilized. Subsequently, 6 mg of the obtained micelles was dissolved in 1 mL of DMSO and 10 μL of a 20 μg/mL NHS-Alexa fluor 647 or maleimide-Alexa fluor C5 568 stock solution in DMSO was added and left to react overnight. Next, the labeled micelles were dialyzed against DMSO and then water and used for the cellular uptake study.

To make sure enough cysteine moieties were available for conjugation of NHS-Alexa fluor 647, micelles with an excess of cysteine moieties (PNC/PNE ratio of 3:2) were made following the same protocol. Conjugation of maleimide-Alexa fluor C5 568 was conducted on micelles formed from the 1:1 molar ratio of PNC and PNE.

Cellular Internalization Study. To investigate the cellular uptake, HeLa and A549 cells were seeded in a glass-bottomed 96 well-plate at a density of 10^4 cells/well and incubated at 37 °C for 24 h. Then, fluorescently labeled micelles were added and incubated with cells at concentrations of 100, 200, and 400 μg/mL for 2, 4, and 24 h at 37 °C. Subsequently, Hoechst 33430 was added to each well 30 min before imaging with a final concentration of 10 nM. The cells were washed twice with PBS and the plate was transferred into a Yokogawa CV7000 (Tokyo, Japan) spinning disk microscope with a 60× 1.2 NA water objective.

Cell Viability Assays. Cytocompatibility of the formed micelles was assessed by MTS assay.[41] HeLa cells were seeded 1 day before the experiment into 96-well plates at a density of 8000 cells/well and were maintained in 200 μL of DMEM low glucose (1 g/L) medium containing 1% antibiotics/antimycotics and 10% FBS for 24 h, at 37 °C. A stock solution of the lyophilized micelles at a concentration of 50 mg/mL in PBS was prepared. The micelle solution was diluted in medium to final concentrations of 1.5, 0.75, 0.375, 0.187, 0.093, 0.046, 0.023, and 0.011 mg/mL. The cells were incubated with the micelles at different concentrations for 24 h. Then, one washing step was performed using PBS and subsequently, 100 μL of fresh medium and 20 μL of MTS reagent was added to the cells and incubated for 2 h. As a negative control group, cells were incubated with 100% culture medium and as a positive control group, cells were incubated in medium containing 1% Triton X-100. The cell viability was determined by measuring the absorbance at 492 nm using a Biochrome EZ microplate reader.

RESULTS AND DISCUSSION

Figure 1 shows the overall synthesis scheme of the two complementary polymers, PNC and PNE, containing cysteine and thioester functional groups, respectively. First, the

DOI: 10.1021/acs.biomac.8b00908
Biomacromolecules 2018, 19, 3766−3775

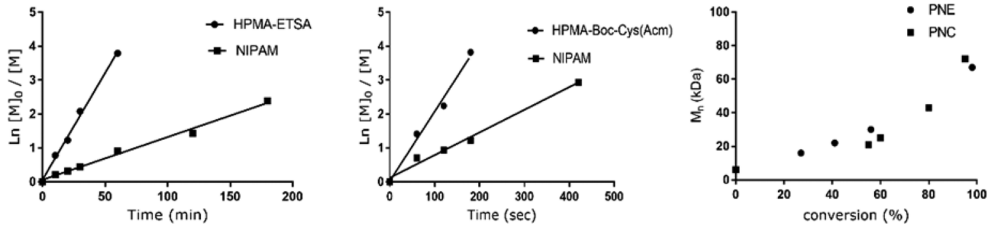

Figure 2. Kinetics of the ATRP of PNE and PNC. (A) $\ln([M]_0/[M])$ as a function of time for the copolymerization of HPMA-ETSA and NIPAM measured by ^{1}H NMR. (B) $\ln([M]_0/[M])$ as a function of time for the copolymerization of HPMA-Boc-Cys(Acm) and NIPAM measured by ^{1}H NMR. $[M]_0$: the initial concentration of monomers (NIPAM/HPMA-Boc-Cys(Acm)/HPMA-ETSA) and [M] concentration of monomers in time (NIPAM/HPMA-Boc-Cys(Acm)/HPMA-ETSA). Polymerization of PNC is significantly faster than polymerization of PNE. (C) Molecular weight evolution of PNC and PNE as a function of monomer conversion. Representative results from one out of three experiments are shown.

Table 1. Characteristics of the Two ABA Triblock Copolymers (PNC and PNE) Synthesized by ATRP[a]

polymer	feed ratio [NIPAM]/[HPMA-Boc-Cys(Acm)]/ HPMA-ETSA]	obtained ratio of [NIPAM]/[HPMA-Boc-Cys(Acm)]/ [HPMA-ETSA][b]	M_n[b] (kDa)	M_n[c] (kDa)	PDI[c]	CP (°C)	yield (%)
PNC	93:7	93:7	42.7	83	1.82	34.1[d]	87
PNE	93:7	92:8	42.1	67	1.72	29.2	81

[a]Both polymers contain PEG mid blocks of 6 kDa with outer blocks composed of either NIPAM and HPMA-Boc-Cys(Acm) (PNC) or NIPAM and HPMA-ETSA (PNE). [b]Determined by ^{1}H NMR. [c]Determined by GPC. [d]Cloud point of deprotected PNC

monomer HPMA-ETSA was designed as comonomer in the thermosensitive blocks of PNE. This monomer was synthesized by conjugation of the hydroxyl group of HPMA to the carboxylic acid functionality of ETSA via a DCC-activated esterification method using DMAP as a catalyst. After column chromatography, the pure monomer was isolated in a yield of 57% and its structure was confirmed by ^{1}H and ^{13}C NMR (SI, Figure 1).

PEG with a number-average molecular weight (M_n) of 6 kDa was completely functionalized at both chain ends with bromoisobutyryl bromide groups. In the next step, this PEG macroinitiator was used for the synthesis of PNC and PNE triblock copolymers by ATRP (Figure 1B,C).

For PNE, the thermosensitive outer blocks consisted of *N*-isopropylacrylamide (NIPAM) and the above-described novel monomer HPMA-ETSA with a ratio of 93:7. The HPMA-ETSA monomer was introduced to obtain a thioester functionality in the thermosensitive domain. After polymerization, the pure polymer was obtained by dialysis and lyophilization in a yield of 81%. The complementary polymer PNC was designed to have a similar structure and size as PNE. Therefore, the same PEG macroinitiator was used for polymerization and a ratio of NIPAM and HPMA-Boc-Cys(Acm) of 93:7 was used. Next, the bromide end groups of PNC polymer chains were substituted by mercaptoethanol to prevent polymer self-cross-linking after deprotection of Boc-cysteine (Acm).[42]

Several methods have been reported for the polymerization of NIPAM in aqueous solutions,[43,44] here for the first time, we introduced an ATRP method for copolymerization of NIPAM and HPMA-Boc-Cys(Acm) or HPMA-ETSA in aqueous solutions. It has been reported before that the polymerization of HPMA can proceed uncontrolled mainly due to complexation of the amine group to the transition-metal complex.[45] Using ligands with a high complexation constant, such as Me_6TREN and the addition of $CuBr_2$ to increase deactivation rate can improve control over the polymerization.[45] In addition, using solvents with the ability to form hydrogen bonds with polymer and monomers reduces the risk of monomer complexation to catalyst.[46]

Figure 2A shows the conversion of monomers during the polymerization of PNE and PNC. For PNE, the residual monomer concentration decreased exponentially over time revealing that the kinetics of polymerization is relatively well-controlled. Moreover, M_n evolved linearly with the conversion which indicates that no significant termination due to recombination occurred (Figure 2C). During the polymerization of PNC, a very fast conversion of HPMA-Boc-Cys(Acm) and NIPAM was observed. The monomer conversion displayed pseudo-first-order kinetics as observed from the linear curves in Figure 2B; however, M_n as a function of conversion did not result in a linear relationship as was observed for PNE (Figure 2C). The higher reactivity of HPMA-Boc-Cys(Acm)/ETSA monomers compared to NIPAM's reactivity during polymerization resulted in a not completely random copolymer having a relatively high HPMA-Boc-Cys(Acm)/ETSA content close to the PEG block. The outer parts of polymeric chains in PNC and PNE are mainly formed of PNIPAM only. The PDIs of the obtained polymers (1.7−1.8) are slightly higher than usually observed for ATRP[47] (Table 1), which can be attributed to the difference in reactivity of acrylamide and methacrylamide monomers, the high length of polymers and the composition of three polymers blocks.[48] A higher M_n determined by GPC compared to NMR is often observed for these kinds of polymers and can be explained by the use of PEGs as GPC standards, which are not perfectly representative polymers to compare hydrodynamic volumes with the synthesized triblock copolymers in the used eluent[49,50] (Table 1).

The cloud point (CP) of PNC prepared by ATRP was 34 °C, which was similar to the CP of a PNC polymer synthesized by free radical polymerization in a previous study (33 °C).[33] As expected, the presence of the more hydrophobic monomer HPMA-ETSA in PNE resulted in a slightly lower CP (29 °C) than the well-known value of 32 °C for homopolymers of PNIPAM[51] (Table 1).

Micelle Characterization. Both PNC and PNE exhibit an increase in solution turbidity above 34.1 and 29.2 °C respectively, indicating lower critical solution temperature (LCST) behavior. Mixing of these polymers at 4 °C, at a

DOI: 10.1021/acs.biomac.8b00908
Biomacromolecules 2018, 19, 3766−3775

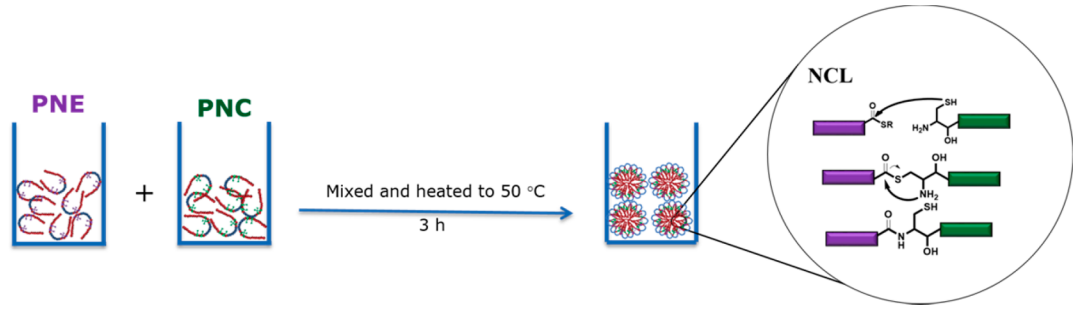

Figure 3. PNC and PNE were dissolved separately in PBS at a concentration of 3 mg/mL at 4 °C and afterward mixed in a 1:1 ratio and immediately heated up to 50 °C using an oil bath. The micellar solution was left at 50 °C for 3 h to let native chemical ligation proceed in the micellar core.

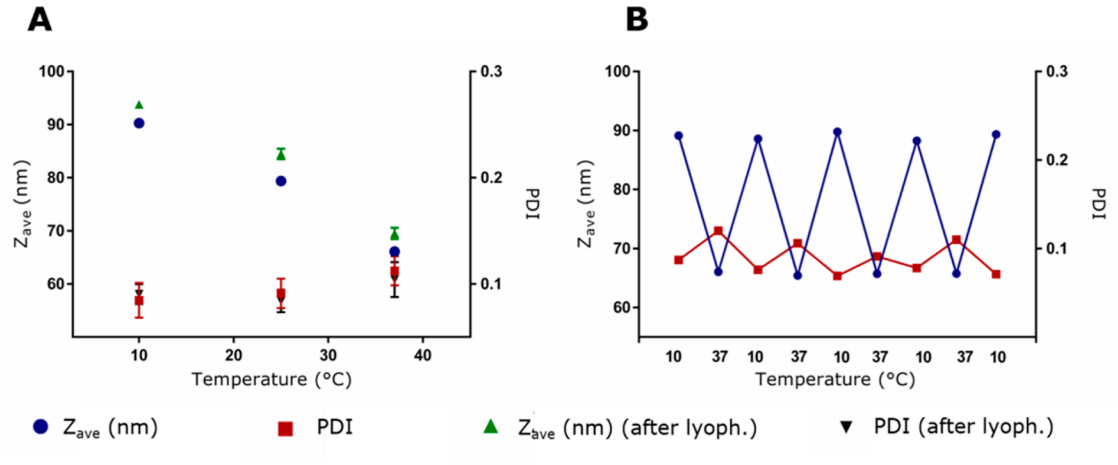

Figure 4. (A) Size of the micelles as a function of temperature, before and after lyophilization. (B) Effect of repeated temperature cycles from 10 to 37 °C on micelle size and PDI.

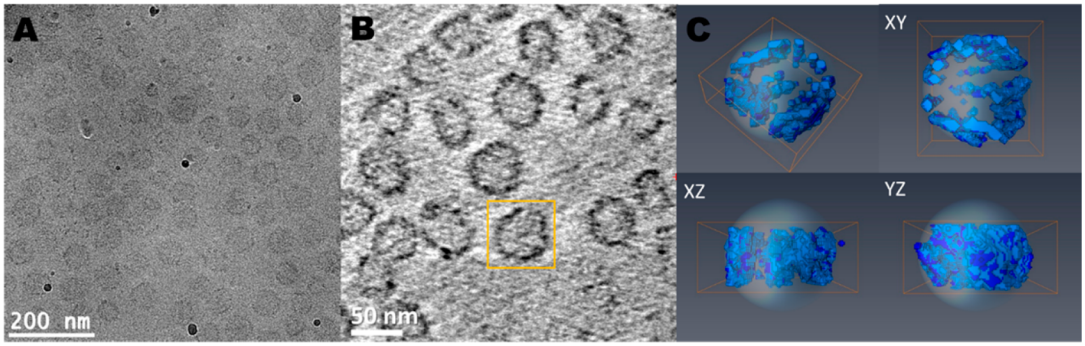

Figure 5. (A) CryoTEM images of uniformly sized spherical micelles at a concentration of 3 mg/mL in water on graphene oxide grid. (B) 5 nm thick tomographic reconstruction of the spherical micelles shown in (A). (C) Cutoff of the tomographic reconstruction of the selected particle from (B) in 3D, *X*–*Y*, *Y*–*Z*, and *X*–*Z* views. The bounding box in (C) is of 55 × 55 × 30 nm^3.

relatively low concentration of 3 mg/mL followed by fast heating (above the LCST of polymers) resulted in dehydration of the outer A-blocks of the polymers and their self-assembly into flower-like micelles (Figure 3). The obtained micelles had a diameter of 65 nm and PDI of 0.11 at 37 °C (Figure 4A), similar to previously reported PNIPAM-PEG-PNIPAM triblock copolymer micelles.[3] Noteworthy, separate solutions of PNC or PNE displayed formation of similar micelles at high temperature, but micelles disappeared immediately upon cooling.

The micellization process brings cysteine and thioester moieties together and facilitates covalent cross-linking of the micellar core by native chemical ligation.[52] To confirm that cross-linking occurred via native chemical ligation (NCL), the formed micelles were passed through a HiTrap desalting column to separate micelles from ethyl thioglycolate, which is the byproduct of the NCL reaction. The Ellman's assay was used to quantify the concentration of released ethyl thioglycolate solution revealing that at least 23% of HPMA-ETSA monomer contributed to cross-linking. Due to the volatile nature of ethyl thioglycolate (boiling point = 54 °C) and, therefore, the partial loss of this compound during the workup, the actual percentage of reacted thioester groups is likely much higher. Moreover, the effectiveness of the cross-

DOI: 10.1021/acs.biomac.8b00908
Biomacromolecules 2018, 19, 3766–3775

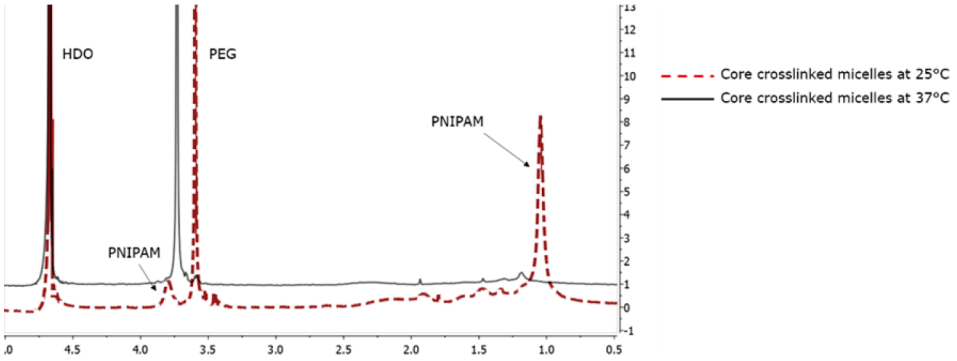

Figure 6. ^{1}H NMR spectra of the core cross-linked micelles in D_2O at 25 and 37 °C. The peak shifts are due to the change in temperature.

linking method was examined by lowering the temperature below the LCST of the PNC and PNE polymers to remove the effect of heat-induced micelle formation.[53] By lowering the temperature below the LCST (10 °C), the size of the micelles increased to a diameter of 90 nm due to rehydration of thermosensitive chains resulting in swelling of the micelles. However, the extent of micelle swelling is limited because of the presence of permanent cross-links. To investigate the reversibility of this behavior, the temperature was changed between 10 and 37 °C repeatedly (below and above LCST of PNE and PNC, respectively). As expected, the size of the micelles changed reversibly as a function of temperature, but notably, the PDI was barely affected (Figure 4B). This "sponge" behavior can be explained by the structure of the polymer as determined from the polymerization kinetics study. According to kinetics study, most HPMA-Cys/ETSA monomers are located next to the PEG chain in both polymers, which results in a cross-linking layer between shell (PEG) and core (PNIPAM segment) of micelles. The PNIPAM segments in the core are relatively flexible and can adjust their conformation depending on temperature resulting in a relatively large difference in size below and above the LCST. The sponge behavior of the micelles is an interesting feature and may be used for loading desirable cargo.

For storage reasons and to remove the released byproduct of NCL, ethyl thioglycolate, the micelles were dialyzed against water and lyophilized. Interestingly, freeze-drying, even without a cryo-protectant, hardly affected the micellar size upon resuspension in buffer (Figure 4A).

The cryoTEM images confirmed the formation of micelles with uniform spherical shape (Figure 5A). The size of micelles reported by this method varies from about 50 to 70 nm, which coincides with the data obtained by DLS. The tomographic view reveals that the polymeric micelles have dark patches mostly located in the corona and some inside the micelle together with lighter areas filling the micellar space (Figure 5B), similar as reported before by Berlepsch et al. for double hydrophobic triblock copolymers.[54] According to an earlier review, the dark patches can be attributed to less hydrated areas in the triblock micelle structure.[55] A close-up of a representative micelle (Figure 5C) shows the distribution of dark patches in the micelle which is unlike the completely dark micellar core that has been observed in, for example, PEO−PB micelles.[56] The surface representation of an extricated micelle (Figure 5C) shows that these patches are distributed throughout the cross-linked space of the micelle. This can be explained by the fact that during polymer synthesis, most HPMA-Cys/ETSA (cross-linkable monomers) were polymerized close to the PEG block. After micellization and cross-linking, these monomers will be located closer to the corona of micelles and form dense and hydrophobic areas which can be seen as dark patches in tomographic view. The low contrast part in the core of micelles could be assigned as the PNIPAM polymeric chains since they remain hydrated at the temperature of sample preparation (room temperature).

These observations are in agreement with the observations of Berlepsch et al. to find patches inside the spherical micelle form instead of a solid single core.[54]

The micelles were studied by ^{1}H NMR in D_2O at 25 and 37 °C, which showed that the signals corresponding to PNIPAM at 1.04 and 3.8 ppm were suppressed by increasing the temperature above the LCST, while the signal corresponding to the protons of PEG at 3.6 ppm remain visible at both temperatures. The disappearance of these characteristic signals confirmed the proposed structure of the micelles with dehydrated PNIPAM hydrophobic cores and hydrated PEG hydrophilic shells (Figure 6).[57]

The micelles' average molecular weight (M_w) and aggregation number (N_{agg}) was measured at different temperatures of 10, 25, 37, and 45 °C by static light scattering (SLS; Table 2). The obtained data by SLS revealed that the micelles'

Table 2. Characteristics of Core Cross-Linked Polymeric Micelles Consisting of PNE and PNC (1:1) Measured by DLS and SLS in PBS

temp (°C)	R_g[a] (nm)	R_h[b] (nm)	R_g/R_h	$M_{w,(mic.)}$ (10^6 Da)	$r_{(mic.)}$[c] (g·cm^{-3})	N_{agg}[d]
10	46.3	48.2	0.95	16.37	0.06	435
25	35.8	42.8	0.84	16.20	0.14	431
37	29.7	35.8	0.83	14.63	0.21	389
45	29.9	35.0	0.85	14.24	0.20	379

[a]Radius of gyration extrapolated to zero concentration. [b]Hydrodynamic radius extrapolated to zero concentration and zero scattering angle. [c]Density of the micelles. [d]Aggregation number of the micelles.

N_{agg} and M_w did not change significantly with increasing temperature. Considering the number of PNE polymers in each micelle according to N_{agg} and cross-link density calculated based on the Ellman's assay, the minimum number of cross-linking points in each micelle is approximately 1000. This number of cross-links corroborates with the high stability of the micelles even at low temperatures.

The ratio of the radius of gyration to the hydrodynamic radius (R_g/R_h) is an important parameter to understand the conformation of the nanoparticles in solution. R_g/R_h values of 0.773, ~1.8, and ~2 have been reported for an uniform sphere,

DOI: 10.1021/acs.biomac.8b00908
Biomacromolecules 2018, 19, 3766−3775

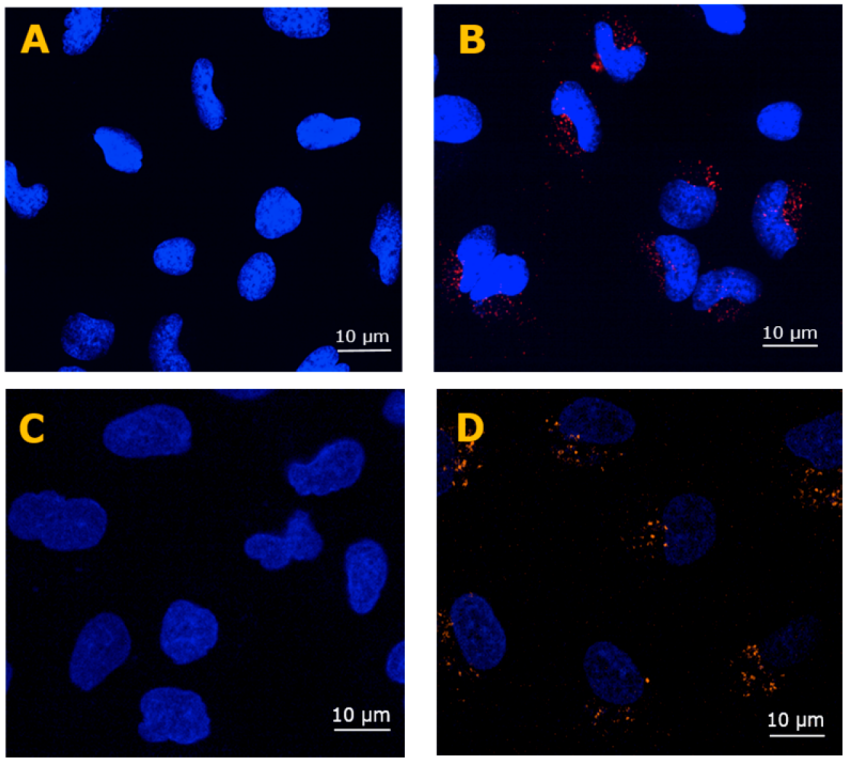

Figure 7. Core cross-linked micelle internalization study. Laser confocal scanning microscopy images of HeLa cells and A549 incubated for 24 h with (A, C) cell culture medium (B, D) fluorescently labeled micelles at a concentration of 400 μg/mL. Cell nuclei are stained with Hoechst (blue) while the micelles are visualized by NHS-Alexa fluor 647 in B (red) and maleimide-Alexa flour C5 568 in D (orange).

a polydisperse linear coil, and a rod-like linear chain, respectively.[58,59] In this study, the found R_g/R_h ratios for the micelles (0.83−0.95) were also similar at the various temperatures and close to the theoretical limit for spherical structures. Furthermore, the increase in the density (r) of micelles with increasing temperature clearly shows shrinking of micelles at temperatures above the LCST of the polymers.

Cell Study. To investigate possible biomedical applications of the developed micelles, cellular uptake was studied on HeLa and A549 cells. To this end, two kinds of dyes which also represent model cargos, having maleimide and amine functionalities, were used for labeling the micelles. An NHS-modified Alexa fluor 647 was used for conjugation to cysteine moieties while a maleimide-modified Alexa fluor C5 568 was used for conjugation to free thiol groups remaining present after native chemical ligation or of nonreacted cysteine moieties. To conjugate NHS modified dyes, micelles with a molar ratio of 3:2 for PNC/PNE were formed. This ratio ensures that sufficient cysteine groups are present in the core of the micelles, which were used for covalent attachment of dye. For the conjugation of maleimide-functionalized dye, micelles with 1:1 molar ratio of PNC and PNE were used. To perform the conjugation, the cross-linked micelles were swollen in DMSO; therefore, cysteine functionalities or thiol moieties became available for conjugation to the dyes. The swelling of micelles in organic solvent did not result in dissociation due to the presence of covalent cross-links and no aggregation was observed after extensive dialysis against water to remove excess dye and solvent. The successful covalent conjugation of these two kinds of dyes demonstrated the accessibility of functional groups in the core of micelles for conjugation to desired cargo molecules having different functional groups.

Cells were incubated with labeled micelles for 2, 4, and 24 h and eventually washed with PBS before imaging. The confocal images in Figure 7 showed punctate fluorescence close to the nuclei confirming the internalization of micelles by cells after 24 h at a concentration of 400 μg/mL. At lower concentrations and shorter incubation times, the presence of micelles inside cells was hardly observed, which can be expected for micelles with PEG corona without targeting ligand.[60]

In addition, cytotoxicity of the micelles was studied on HeLa cells. An MTS assay was performed to assess the metabolic activity of cells in the presence of the micelles. In living cells, mitochondrial enzymes reduce the MTS tetrazolium compound and generate a colored formazan that can be quantified by a colorimetric method.[61] Figure 8 shows that no change in mitochondrial activity was observed upon incubation of HeLa cells with micelles at concentrations ranging from 11 μg/mL to 1.5 mg/mL after 24 h. To study possible cell membrane damage upon exposure to the micelles, an LDH assay was performed. In damaged cells, lactate dehydrogenase (LDH) is released, which catalyzes a series of reactions that eventually cause reduction of a tetrazolium salt to a highly colored formazan, which absorbs strongly at 490−520 nm.[62] The results demonstrated no damage to the cell membrane upon incubation with micelles over a wide range of concentrations (SI, Figure 5). These results confirm the cytocompatibility of these micelles.

CONCLUSION

In this study, native chemical ligation was introduced as a mild, chemoselective method for the cross-linking of micelles in an

DOI: 10.1021/acs.biomac.8b00908
Biomacromolecules 2018, 19, 3766−3775

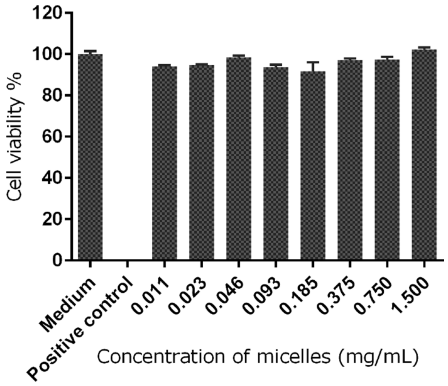

Figure 8. In vitro cytotoxicity (MTS assay) on HeLa cells after 24 h incubation with micelles across a 135-fold concentration range (0.011−1.5 mg/mL). Data are presented as mean values ± SD of three independent experiments.

aqueous medium. Mixing two complementary PNIPAM-based ABA polymers, containing either HPMA-Cys or HPMA-ETSA, and subsequently, increasing the temperature above the LCST resulted in flower-like micelles with a size of 65 nm at 37 °C. Reducing the temperature to 10 °C resulted in a change in the size of the micelles to 90 nm, but hardly showed any change in polydispersity and aggregation number, thus, confirming permanent cross-linking of the micelles. The uniform spherical shape of micelles was confirmed by cryo-TEM. Interestingly, in tomographic view of the micelles, dark patches were seen close to the corona of micelles, which according to the kinetics study corresponds to the area with the highest content of cross-linkable monomers. Therefore, the dark patches can be interpreted as the cross-linked area of the micelles while the inner low contrast part of micelles is composed of the more hydrated PNIPAM chains. In addition, by adjusting the molar ratio between PNC and PNE polymers during micelle formation, nucleophilic (cysteine) or electrophilic (thioester) sites can be introduced within the micellar core. Here, we have shown that the presence of cysteine and thiol moieties remaining after cross-linking could be used for conjugation of an NHS or maleimide functionalized dyes, respectively. These functional sites may also be used for further modification of the micelle to introduce (pro) drugs or charge in the core. Notably, this cross-linking method resulting in the presence of thiol moieties in the micellar core also provides the possibility for conjugation of cargo via a disulfide bond, which may be interesting for intracellular drug delivery. Moreover, the high cell viability and observed cellular uptake of these micelles by HeLa cells show a good cytocompatibility profile and potential of this nanocarrier for drug delivery applications.

■ ASSOCIATED CONTENT

Supporting Information

The Supporting Information is available free of charge on the ACS Publications website at DOI: 10.1021/acs.biomac.8b00908.

NMR spectra (^{1}H and ^{13}C NMR) of HPMA-ETSA (Figure 1A,B); ^{1}H NMR spectrum of PNE (Figure 2); ^{1}H NMR spectrum of PNC (Figure 3); GPC chromatograms of PNE and PNC (Figure 4A,B); and LDH assay on HeLa cells (Figure 5) (PDF).

■ AUTHOR INFORMATION

Corresponding Author

*E-mail: t.vermonden@uu.nl

ORCID

Mohammad-Amin Moradi: 0000-0003-3754-9200
Heiner Friedrich: 0000-0003-4582-0064
Nico A. J. M. Sommerdijk: 0000-0002-8956-195X
Mathew Hembury: 0000-0002-7949-0027
Tina Vermonden: 0000-0002-6047-5900

Notes

The authors declare no competing financial interest.

■ ACKNOWLEDGMENTS

Netherlands Organization for Scientific Research (NWO/VIDI 13457 and NWO/Aspasia 015.009.038) is acknowledged for funding.

■ REFERENCES

(1) Miyata, K.; Christie, R. J.; Kataoka, K. *React. Funct. Polym.* **2011**, *71* (3), 227−234.
(2) Shi, Y.; van Nostrum, C. F.; Hennink, W. E. *ACS Biomater. Sci. Eng.* **2015**, *1* (6), 393−404.
(3) De Graaf, A. J.; Boere, K. W. M.; Kemmink, J.; Fokkink, R. G.; Van Nostrum, C. F.; Rijkers, D. T. S.; Van Der Gucht, J.; Wienk, H.; Baldus, M.; Mastrobattista, E.; Vermonden, T.; Hennink, W. E. *Langmuir* **2011**, *27*, 9843−9848.
(4) Liu, B.; Chen, H.; Li, X.; Zhao, C.; Liu, Y.; Zhu, L.; Deng, H.; Li, J.; Li, G.; Guo, F.; Zhu, X. *RSC Adv.* **2014**, *4* (90), 48943−48951.
(5) Sprakel, J.; Besseling, N. A. M.; Cohen Stuart, M. A.; Leermakers, F. A. M. *Eur. Phys. J. E: Soft Matter Biol. Phys.* **2008**, *25* (2), 163−173.
(6) Oh, K. T.; Oh, Y. T.; Oh, N.; Kim, K.; Lee, D. H.; Lee, E. S. *Int. J. Pharm.* **2009**, *375* (1−2), 163−169.
(7) Lee, E. S.; Oh, K. T.; Kim, D.; Youn, Y. S.; Bae, Y. H. *J. Controlled Release* **2007**, *123* (1), 19−26.
(8) Lee, W.-C.; Li, Y.-C.; Chu, I.-M. *Macromol. Biosci.* **2006**, *6* (10), 846−854.
(9) Matyjaszewski, K.; Xia, J. *Chem. Rev.* **2001**, *101*, 2921−2990.
(10) Jankova, K.; Chen, X.; Kops, J.; Batsberg, W. *Macromolecules* **1998**, *31* (2), 538−541.
(11) Boyer, C.; Corrigan, N. A.; Jung, K.; Nguyen, D.; Nguyen, T.-K.; Adnan, N. N. M.; Oliver, S.; Shanmugam, S.; Yeow, J. *Chem. Rev.* **2016**, *116* (4), 1803−1949.
(12) Gref, R.; Lück, M.; Quellec, P.; Marchand, M.; Dellacherie, E.; Harnisch, S.; Blunk, T.; Müller, R. H. *Colloids Surf., B* **2000**, *18* (3−4), 301−313.
(13) Kataoka, K.; Harada, A.; Nagasaki, Y. *Adv. Drug Delivery Rev.* **2012**, *64* (SUPPL), 37−48.
(14) Talelli, M.; Rijcken, C. J. F.; Hennink, W. E.; Lammers, T. *Curr. Opin. Solid State Mater. Sci.* **2012**, *16* (6), 302−309.
(15) Talelli, M.; Barz, M.; Rijcken, C. J. F.; Kiessling, F.; Hennink, W. E.; Lammers, T. *Nano Today* **2015**, *10*, 93−117.
(16) Iijima, M.; Nagasaki, Y.; Okada, T.; Kato, M.; Kataoka, K. *Macromolecules* **1999**, *32* (4), 1140−1146.
(17) Siegwart, D. J.; Whitehead, K. A.; Nuhn, L.; Sahay, G.; Cheng, H.; Jiang, S.; Ma, M.; Lytton-Jean, A.; Vegas, A.; Fenton, P.; Levins, C. G.; Love, K. T.; Lee, H.; Cortez, C.; Collins, S. P.; Li, Y. F.; Jang, J.; Querbes, W.; Zurenko, C.; Novobrantseva, T.; Langer, R.; Anderson, D. G. *Proc. Natl. Acad. Sci. U. S. A.* **2011**, *108* (32), 12996−13001.
(18) Bronich, T. K.; Keifer, P. A.; Shlyakhtenko, L. S.; Kabanov, A. V. *J. Am. Chem. Soc.* **2005**, *127*, 8236−8237.
(19) Kim, J. O.; Sahay, G.; Kabanov, A. V.; Bronich, T. K. *Biomacromolecules* **2010**, *11* (4), 919−926.
(20) Zhang, Z.; Yin, L.; Tu, C.; Song, Z.; Zhang, Y.; Xu, Y.; Tong, R.; Zhou, Q.; Ren, J.; Cheng, J. *ACS Macro Lett.* **2013**, *2* (1), 40−44.

DOI: 10.1021/acs.biomac.8b00908
Biomacromolecules 2018, 19, 3766−3775

(21) Jiang, X.; Zheng, Y.; Chen, H. H.; Leong, K. W.; Wang, T.-H.; Mao, H.-Q. *Adv. Mater.* **2010**, *22* (23), 2556−2560.
(22) Li, Y.; Xiao, K.; Luo, J.; Xiao, W.; Lee, J. S.; Gonik, A. M.; Kato, J.; Dong, T. A.; Lam, K. S. *Biomaterials* **2011**, *32* (27), 6633−6645.
(23) Fu, R.; Fu, G.-D. *Polym. Chem.* **2011**, *2*, 465−475.
(24) Lowe, A. B. *Polym. Chem.* **2014**, *5* (17), 4820−4870.
(25) O'Reilly, R. K.; Joralemon, M. J.; Hawker, C. J.; Wooley, K. L. *New J. Chem.* **2007**, *31* (5), 718−724.
(26) Zhang, J.; Zhou, Y.; Zhu, Z.; Ge, Z.; Liu, S. *Macromolecules* **2008**, *41* (4), 1444−1454.
(27) Xia, Y.; He, H.; Liu, X.; Hu, D.; Yin, L.; Lu, Y.; Xu, W. *Polym. Chem.* **2016**, *7* (41), 6330−6339.
(28) Bapat, A. P.; Ray, J. G.; Savin, D. A.; Hoff, E. A.; Patton, L.; Sumerlin, B. S. Dynamic-covalent Nanostructures Prepared by Diels−Alder Reactions of Styrene-maleic anhydride-derived Copolymers Obtained by One-step Cascade Block Copolymerization. *Polym. Chem.* **2012**, *3*, 3112−3120.
(29) Huang, Y.; Sun, R.; Luo, Q.; Wang, Y.; Zhang, K.; Deng, X.; Zhu, W.; Li, X.; Shen, Z. In situ fabrication of paclitaxel-loaded core-cross-linked micelles via thiol-ene "click" chemistry for reduction-responsive drug release. *J. Polym. Sci., Part A: Polym. Chem.* **2016**, *54*, 99−107.
(30) Johnson, E. C. B.; Kent, S. B. H. *J. Am. Chem. Soc.* **2006**, *128* (20), 6640−6646.
(31) Hu, B.-H.; Su, J.; Messersmith, P. B. *Biomacromolecules* **2009**, *10*, 2194−2200.
(32) Boere, K. W. M.; van den Dikkenberg, J.; Gao, Y.; Visser, J.; Hennink, W. E.; Vermonden, T. *Biomacromolecules* **2015**, *16*, 2840−2851.
(33) Boere, K. W. M.; Soliman, B. G.; Rijkers, D. T. S.; Hennink, W. E.; Vermonden, T. *Macromolecules* **2014**, *47*, 2430−2438.
(34) Zhou, Z.; Chu, B. *Macromolecules* **1994**, *27* (8), 2025−2033.
(35) *Temperature-Responsive Polymers: Chemistry, Properties and Applications*; Khutoryanskiy, V. V., T. K. G, Eds.; John Wiley & Sons, Inc., 2018.
(36) Ulbrich, K.; Šubr, V.; Strohalm, J.; Plocová, D.; Jelínková, M.; Říhová, B. *J. Controlled Release* **2000**, *64* (1−3), 63−79.
(37) Loccufier, J.; Van Bos, M.; Schacht, E. *Polym. Bull.* **1991**, *27* (2), 201−204.
(38) Patterson, J. P.; Xu, Y.; Moradi, M.-A.; Sommerdijk, N. A. J. M.; Friedrich, H. *Acc. Chem. Res.* **2017**, *50* (7), 1495−1501.
(39) van de Put, M. W. P.; Patterson, J. P.; Bomans, P. H. H.; Wilson, N. R.; Friedrich, H.; van Benthem, R. A. T. M.; de With, G.; O'Reilly, R. K.; Sommerdijk, N. A. J. M. *Soft Matter* **2015**, *11* (7), 1265−1270.
(40) Wirix, M. J. M.; Bomans, P. H. H.; Hendrix, M. M. R. M.; Friedrich, H.; Sommerdijk, N. A. J. M.; de With, G. *J. Mater. Chem. A* **2015**, *3* (9), 5031−5040.
(41) Malich, G.; Markovic, B.; Winder, C. *Toxicology* **1997**, *124* (3), 179−192.
(42) Tsarevsky, N. V.; Matyjaszewski, K. *Macromolecules* **2002**, *35* (24), 9009−9014.
(43) de Graaf, A. J.; Mastrobattista, E.; Vermonden, T.; van Nostrum, C. F.; Rijkers, D. T. S.; Liskamp, R. M. J.; Hennink, W. E. *Macromolecules* **2012**, *45* (2), 842−851.
(44) Zhang, Q.; Wilson, P.; Li, Z.; McHale, R.; Godfrey, J.; Anastasaki, A.; Waldron, C.; Haddleton, D. M. *J. Am. Chem. Soc.* **2013**, *135* (19), 7355−7363.
(45) Teodorescu, M.; Matyjaszewski, K. *Macromolecules* **1999**, *32* (15), 4826−4831.
(46) Xia, Y.; Yin, X.; Burke, N. a D.; Stover, H. D. H. *Macromolecules* **2005**, *38*, 5937−5943.
(47) Masci, G.; Giacomelli, L.; Crescenzi, V. *Macromol. Rapid Commun.* **2004**, *25*, 559−564.
(48) *Handbook of Radical Polymerization*; Matyjaszewski, K., Davis, T. P., Eds.; John Wiley & Sons, Inc.: Hoboken, NJ, U.S.A., 2002.
(49) Smithenry, D. W.; Kang, M.-S.; Gupta, V. K. *Macromolecules* **2001**, *34* (24), 8503−8511.
(50) Su, W.-F. *Principles of Polymer Design and Synthesis*; Lecture Notes in Chemistry; Springer: Berlin, Heidelberg, 2013; Vol. *82*.
(51) Schild, H. G. *Prog. Polym. Sci.* **1992**, *17*, 163−249.
(52) Dawson, P. E.; Kent, S. B. H. *Annu. Rev. Biochem.* **2000**, *69* (1), 923−960.
(53) Wei, H.; Cheng, S.-X.; Zhang, X.-Z.; Zhuo, R.-X. *Prog. Polym. Sci.* **2009**, *34*, 893−910.
(54) Berlepsch, H. v.; Böttcher, C.; Skrabania, K.; Laschewsky, A. *Chem. Commun.* **2009**, No. 17, 2290.
(55) Holder, S. J.; Sommerdijk, N. A. J. M. *Polym. Chem.* **2011**, *2* (5), 1018.
(56) Zheng, Y.; Won, Y.-Y.; Bates, F. S.; Davis, H. T.; Scriven, L. E.; Talmon, Y. *J. Phys. Chem. B* **1999**, *103* (47), 10331−10334.
(57) Soga, O.; van Nostrum, C. F.; Ramzi, A.; Visser, T.; Soulimani, F.; Frederik, P. M.; Bomans, P. H. H.; Hennink, W. E. *Langmuir* **2004**, *20* (21), 9388−9395.
(58) Aharoni, S. M.; Murthy, N. S. *Polym. Commun.* **1983**, *24* (5), 132−136.
(59) Van de Sande, W.; Persoons, A. *J. Phys. Chem.* **1985**, *89* (3), 404−406.
(60) Mishra, S.; Webster, P.; Davis, M. E. *Eur. J. Cell Biol.* **2004**, *83* (3), 97−111.
(61) Berridge, M. V.; Herst, P. M.; Tan, A. S. *Biotechnol. Annu. Rev.* **2005**, *11*, 127−152.
(62) Khattak, S. F.; Spatara, M.; Roberts, L.; Roberts, S. C. *Biotechnol. Lett.* **2006**, *28* (17), 1361−1370.

DOI: 10.1021/acs.biomac.8b00908
Biomacromolecules 2018, 19, 3766−3775